Supporting Information

Synergistic Effects of Heteroatom decorated MXene catalyst for CO Reduction Reaction

Lei Li, [1,2,3] Baihai Li,[1] Haoran Guo,[4] Yanle Li,[2] Chenghua Sun, [5,6] Ziqi Tian,*[,2,3] Liang Chen*[,2,3]

[1] School of Materials and Energy, University of Electronic Science and Technology of China, Chengdu 611731, Sichuan, China

[2] Ningbo Institute of Materials Technology and Engineering, Chinese Academy of Sciences, Ningbo 315201, Zhejiang, China

[3] University of Chinese Academy of Sciences, 100049, Beijing, China

[4]School of Chemical Sciences, University of Chinese Academy of Sciences, Beijing, 100049, China

[5]Department of Chemistry and Biotechnology, Faculty of Science, Engineering & Technology, Swinburne University of Technology, Hawthorn, VIC 3122, Australia

[6]School of Chemical Engineering and Energy Technology, Dongguan University of Technology, Dongguan 523808, PR China

Email: tianziqi@nimte.ac.cn; chenliang@nimte.ac.cn

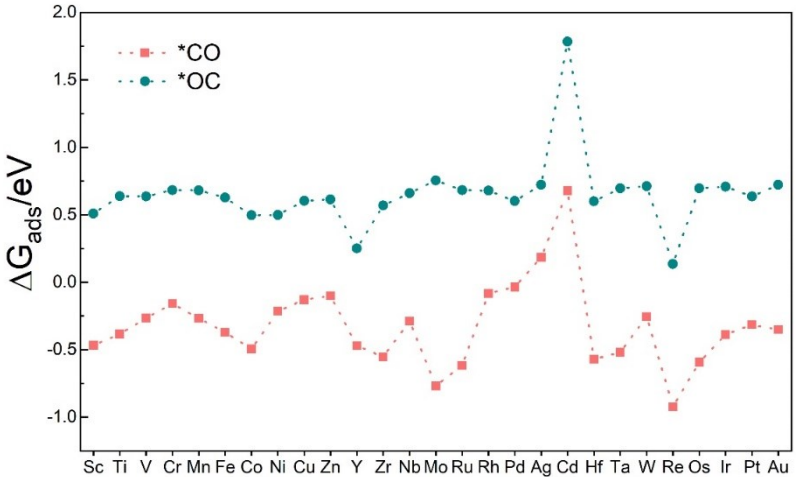

Figure S1. Adsorption free energy comparison between *CO and *OC on TM-HACs.

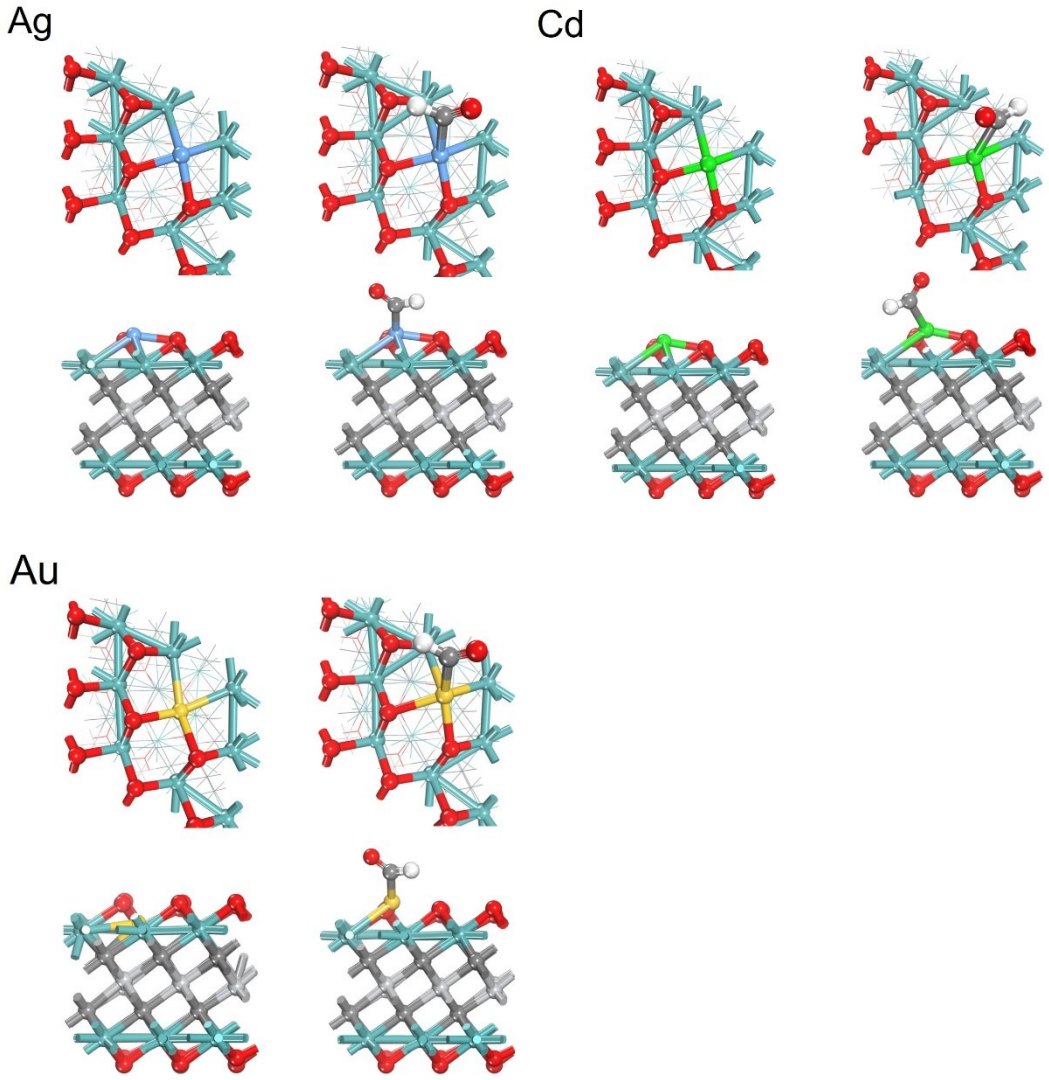

Figure S2. Top and side view of pristine and *CHO on TM-HACs, where Ag, Cd and Au atoms are drawn in blue, green and yellow.

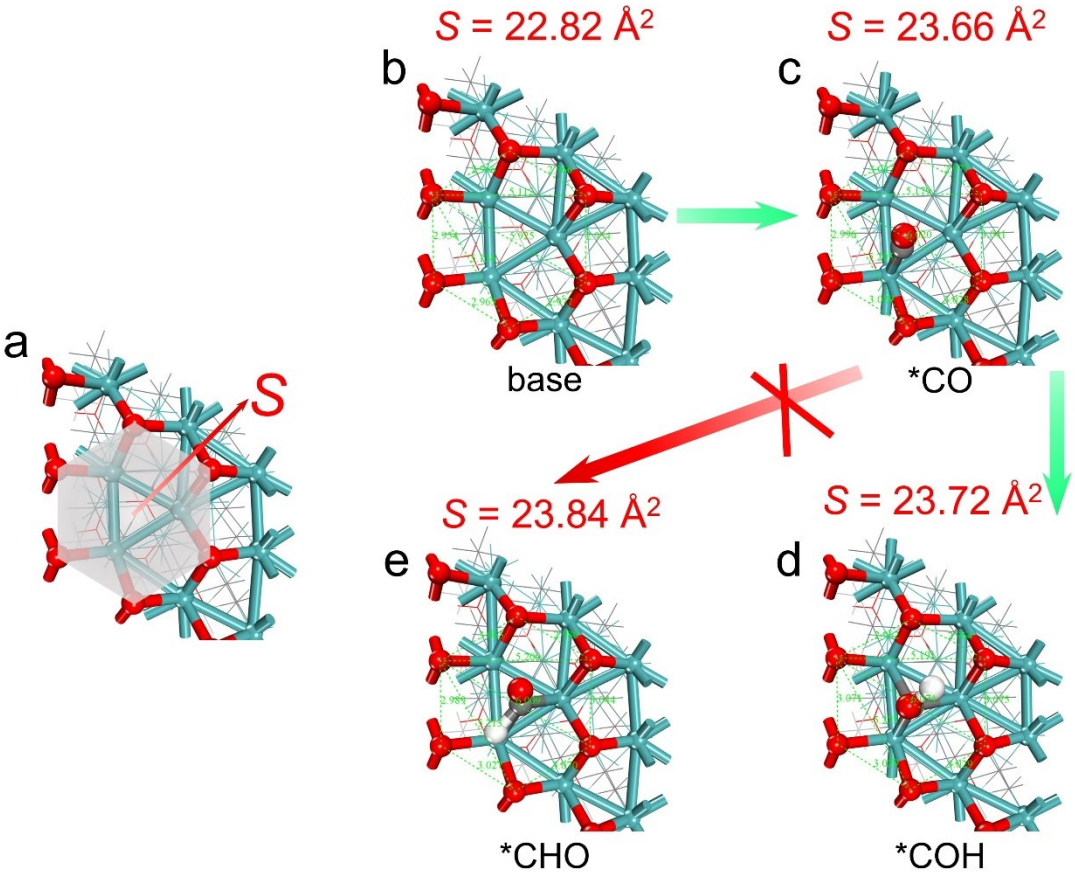

Figure S3. (a) The top view of Mo-HAC, where the *S* represents the area enclosed by six Oxygen atoms near heteroatom active center. They are 22.82, 23.66, 23.72 and 23.84 Å^2 for pristine, *CO, *COH and *CHO Mo-HAC, respectively.

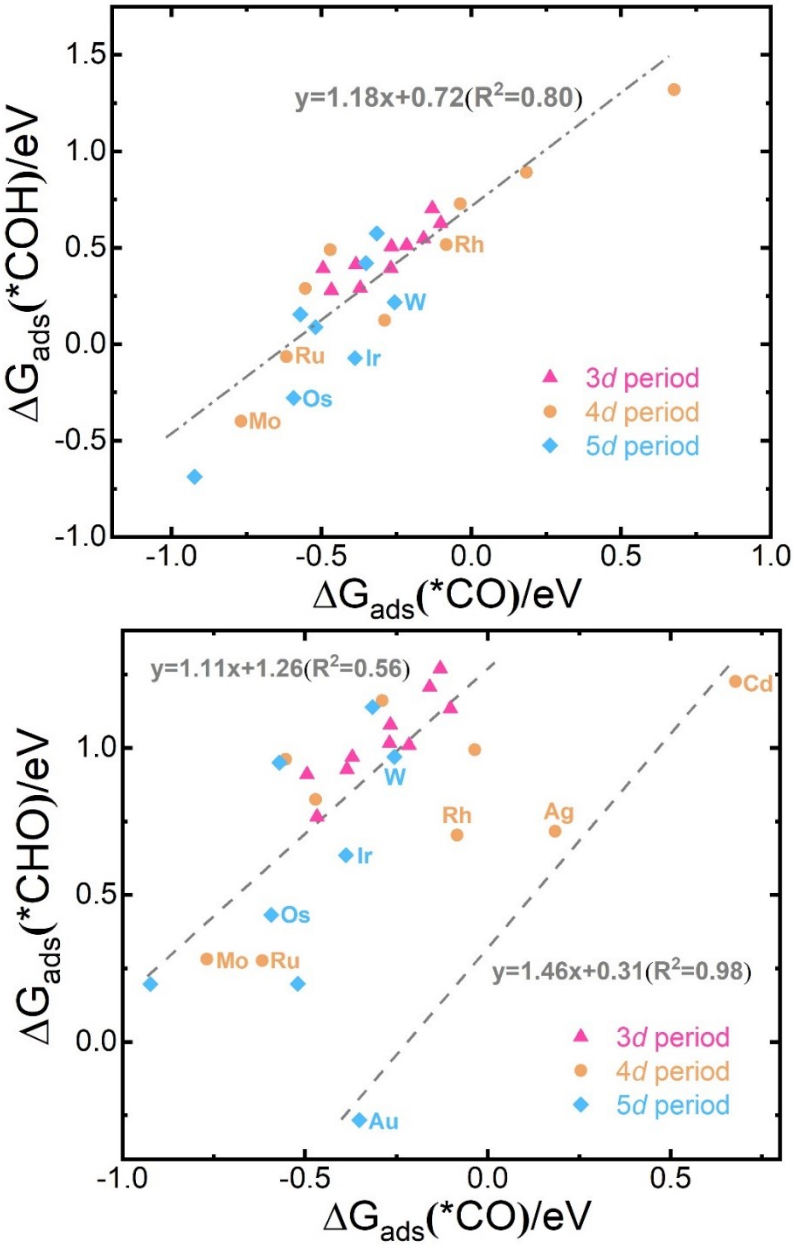

Figure S4. The scaling relationships between ΔG_{ads}(*CO) and ΔG_{ads}(*COH) or ΔG_{ads}(*CHO), respectively.

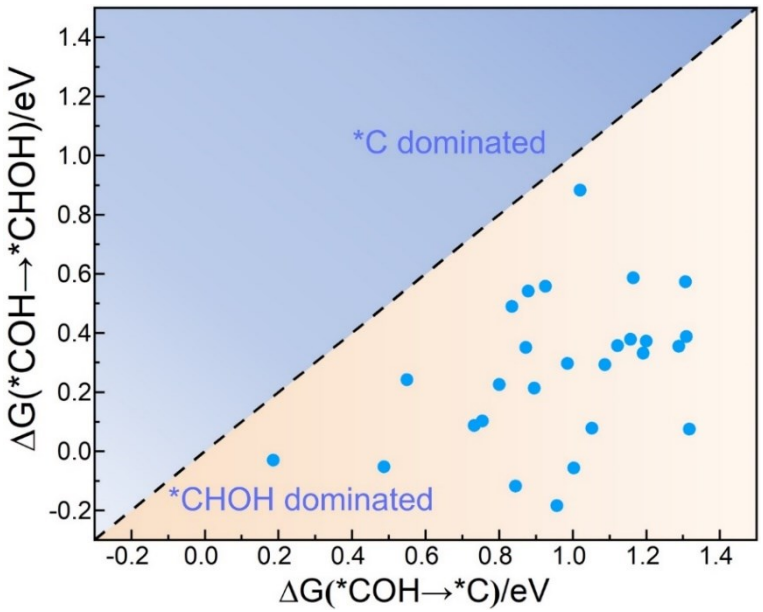

Figure S5. Reaction free energy comparison between ΔG(*COH→*C) and ΔG(*COH→*CHOH).

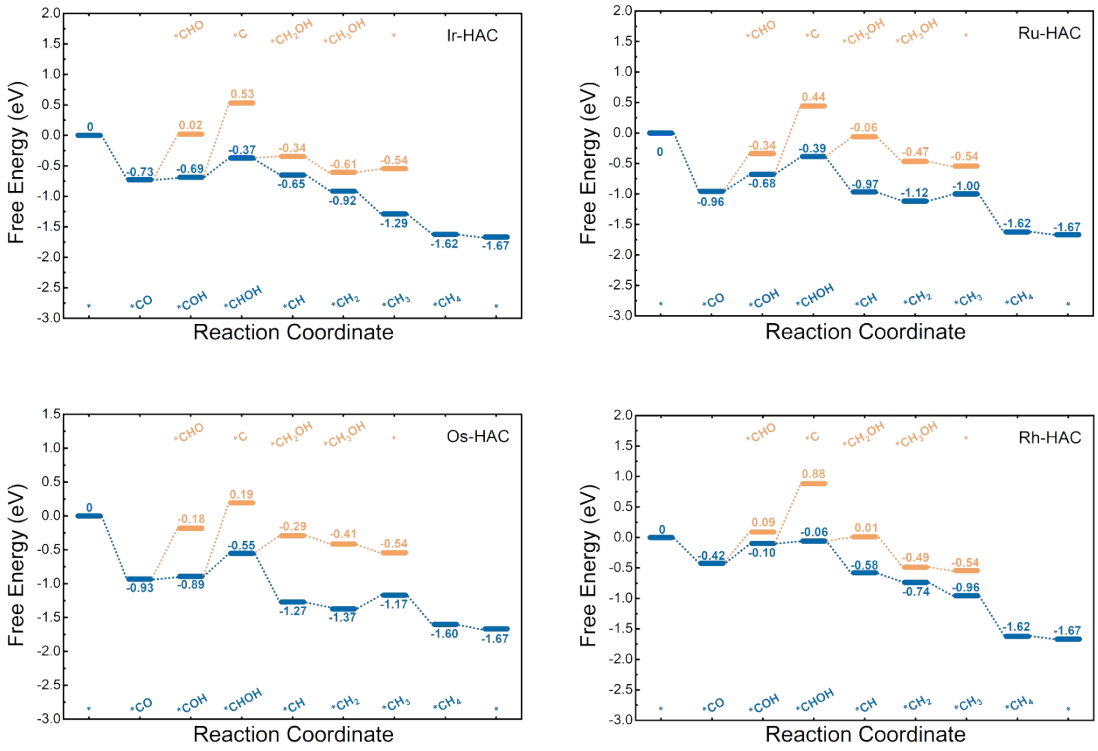

Figure S6. Free energy diagram for CORR with all possible reaction intermediates on Ir, Ru, Os, and Rh-HAC, respectively. The energetically favorite route was drawn in blue, and yellow for the undesirable products.

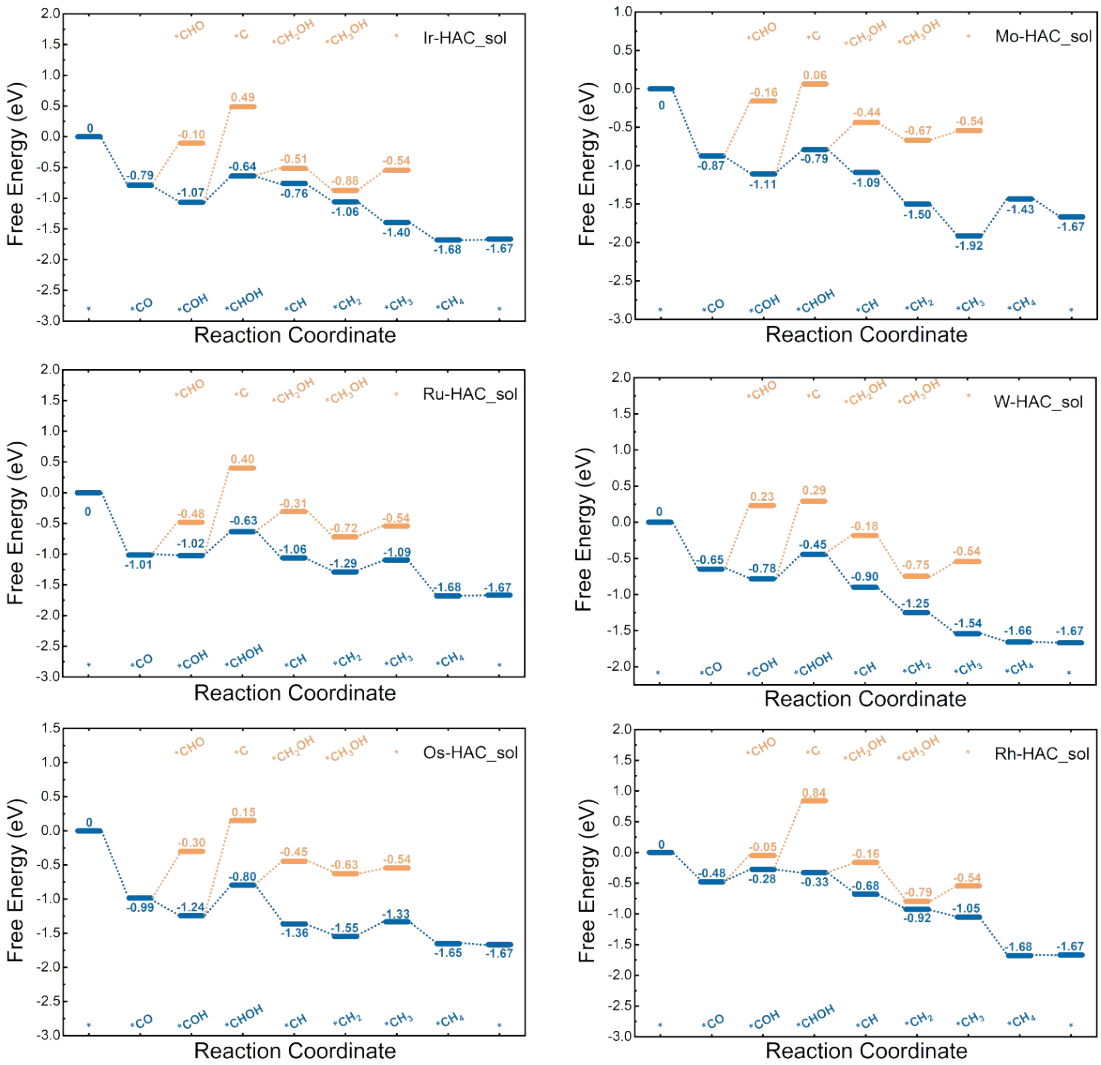

Figure S7. Free energy diagram for CORR under solvation condition with all possible reaction intermediates on Ir, Mo, Ru, W, Os, and Rh-HAC, respectively. The energetically favorite route was drawn in blue, and yellow for the undesirable products.

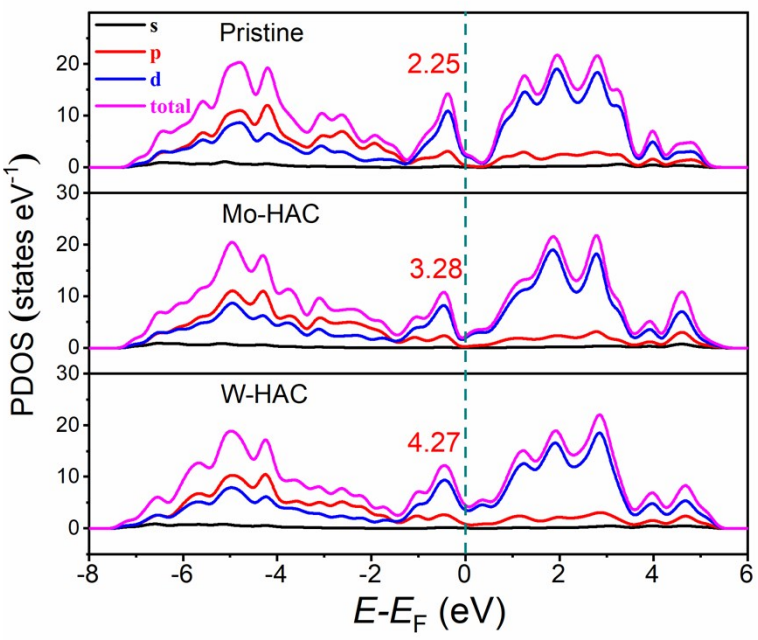

Figure S8. The calculated projected DOSs of pristine $Mo_2TiC_2O_2$ layer, Mo-HAC, and W-HAC.

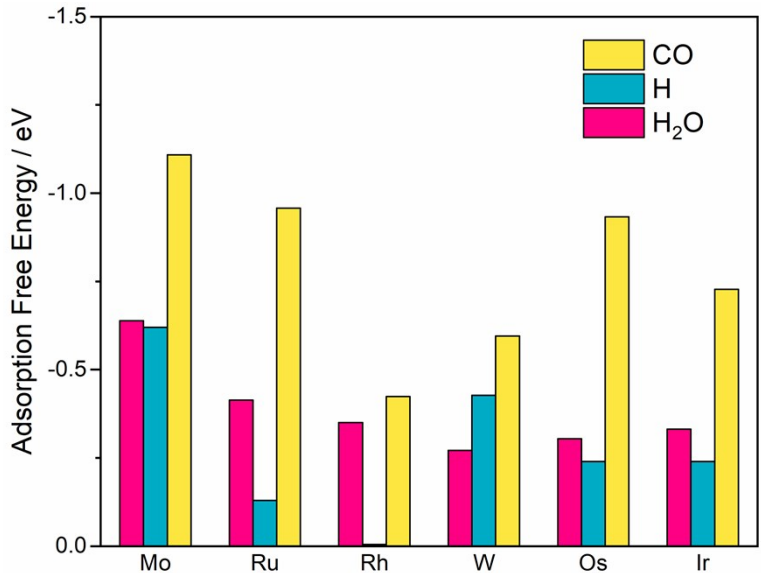

Figure S9. Comparison adsorption free energies of H_2O, H, and CO on the selected candidates.

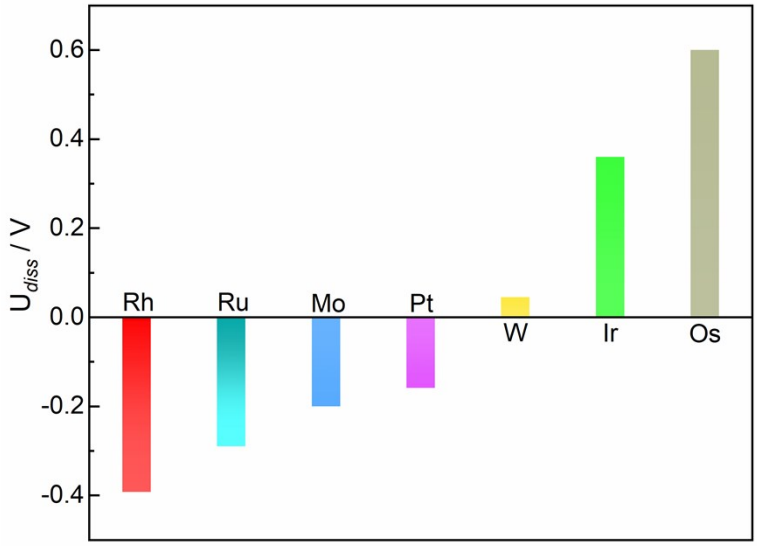

Figure S10. DFT calculated dissolution potentials (U_{diss}) of these selected candidates, comparing with that of the synthesized Pt-HAC.

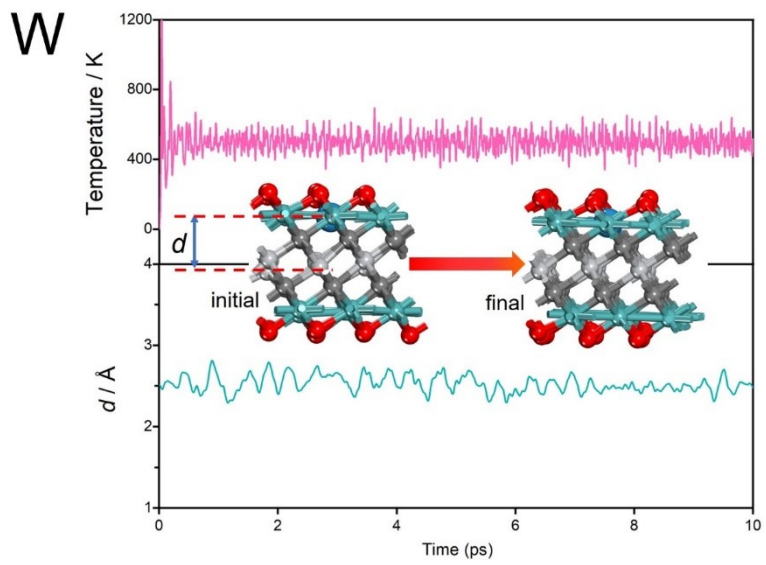
W
Temperature / K
1200
800
400
0
d
initial
final
4
3
d / Å
2
1
0
2
4
6
8
10
Time (ps)

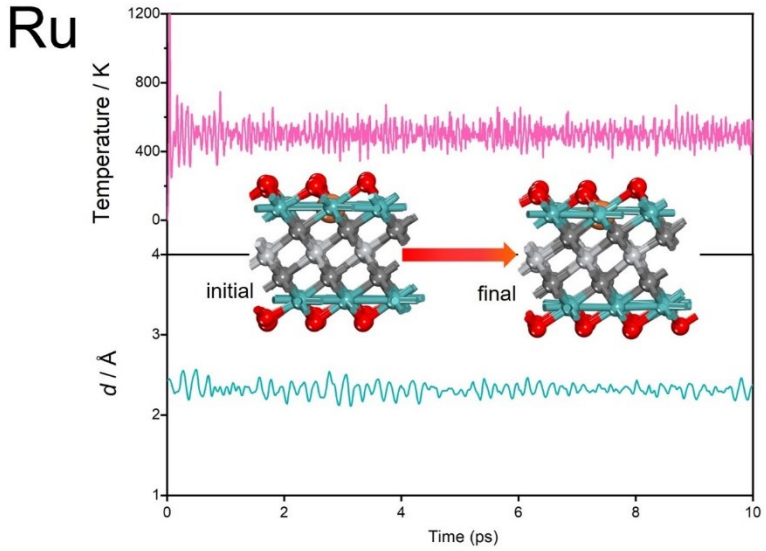
Ru
Temperature / K
1200
800
400
0
initial
final
4
3
d / Å
2
1
0
2
4
6
8
10
Time (ps)

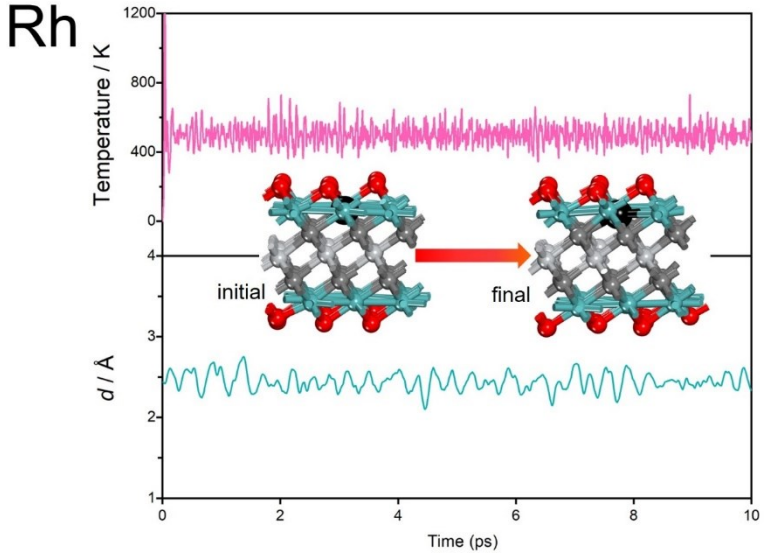
Rh
Temperature / K
1200
800
400
0
initial
final
4
3
d / Å
2
1
0
2
4
6
8
10
Time (ps)

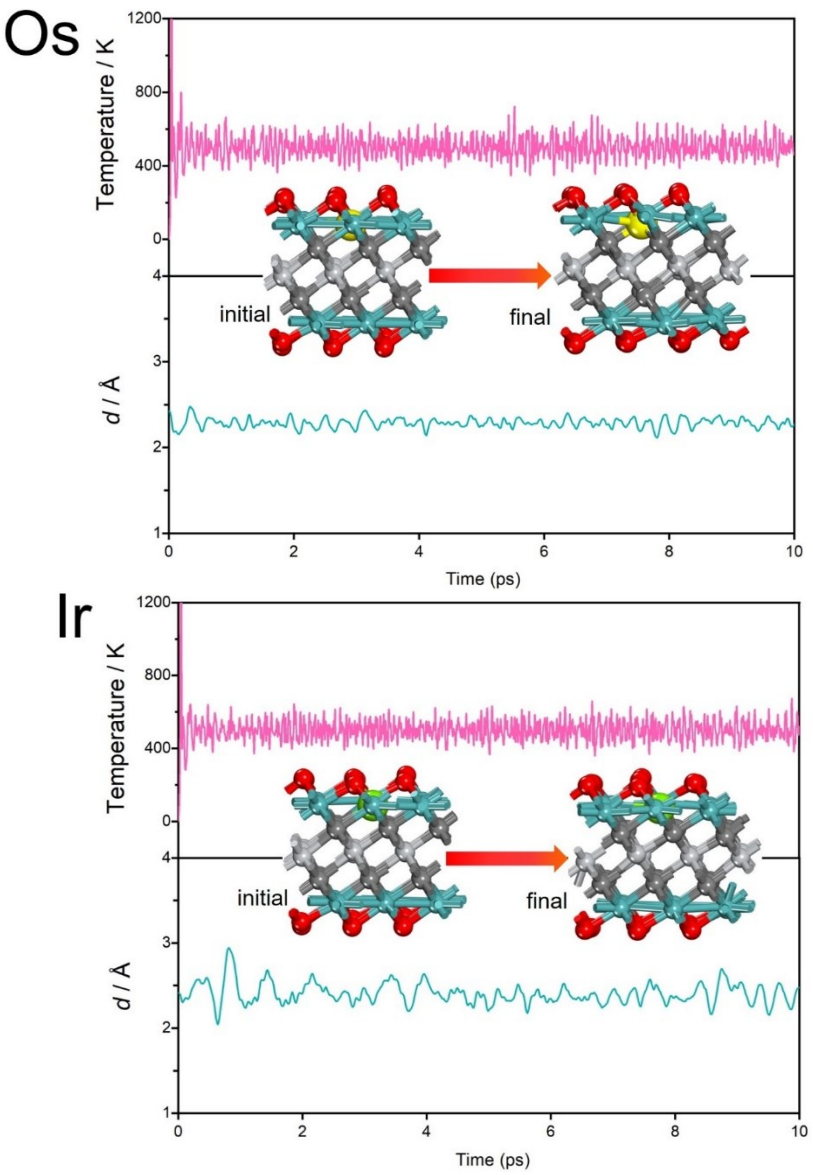

Figure S11. Fluctuation of temperature and distance between anchor TM and the middle Ti-layer (*d*) versus time for TM-HACs, respectively. The snapshots at the beginning and the end of the trajectory are also shown.

Table S1 Calculated ZPE and TS energies for different species, where the label * denotes the status of adsorption.

Adsorbed species	E_{ZPE} (eV)	E_{TS} (eV)
CO	0.14	0.62
H_2	0.27	0.41
H_2O	0.60	0.59
CH_4	1.19	0.57
CH_3OH	1.37	0.74
***CO**	0.21	0.12
***COH**	0.50	0.12
***CHO**	0.44	0.13
***C**	0.10	0.02
***CHOH**	0.80	0.10
***CH**	0.35	0.05
***CH_2**	0.62	0.06
***CH_3**	0.94	0.08
***CH_4**	1.20	0.27
***CH_2OH**	1.08	0.17
***CH_3OH**	1.36	0.21